

Article

# Energy-Efficient Access Point Selection Scheme for Reconfigurable-Intelligent-Surface-Assisted Cell-Free Massive MIMO Systems

Weiran Wang , Jiaqi Song and Jianguo Zhou

School of Electronic Information, Wuhan University, Wuhan 430072, China; songjq@whu.edu.cn (J.S.)

\* Correspondence: wangweiran@whu.edu.cn; Tel.: +86-181-6156-3829

**Abstract:** Reconfigurable intelligent surface (RIS)-assisted cell-free (CF) massive Multiple-Input Multiple-Output (MIMO) technology exhibits significant potential in enhancing the energy efficiency of 6G mobile communications. Nevertheless, recent studies suggest that both access points (APs) and RISs encounter challenges related to a high energy consumption during operation. To address this issue, strategies involving AP hibernation and RIS shut-off are proposed. Subsequently, an optimization problem is formulated to jointly optimize RISs, beamforming vectors, and AP selection with the aim of maximizing the energy efficiency (EE). Initially, the non-convex optimization problem for maximizing energy efficiency is decomposed into three sub-problems. These sub-problems are subsequently reformulated using fractional programming and variational programming techniques and then solved using the successive convex approximation (SCA) algorithm, Dinkelbach algorithm, and greedy algorithm, respectively. Subsequently, an alternate optimization algorithm based on block gradient descent is introduced to iteratively solve the four-variable optimization problem, thereby obtaining an approximate solution to the original problem. The simulation results demonstrate that the algorithm significantly reduces energy consumption. Specifically, compared to the scheme without the hibernation strategy, the energy efficiency (EE) is enhanced by 35%.

**Keywords:** RIS; CF; massive MIMO; AP hibernation; RIS turn-off; energy efficiency



**Citation:** Wang, W.; Song, J.; Zhou, J. Energy-Efficient Access Point Selection Scheme for Reconfigurable-Intelligent-Surface-Assisted Cell-Free Massive MIMO Systems. *Electronics* **2024**, *13*, 1397. <https://doi.org/10.3390/electronics13071397>

Academic Editor: Federico Alimenti

Received: 7 March 2024

Revised: 30 March 2024

Accepted: 3 April 2024

Published: 7 April 2024



**Copyright:** © 2024 by the authors. Licensee MDPI, Basel, Switzerland. This article is an open access article distributed under the terms and conditions of the Creative Commons Attribution (CC BY) license (<https://creativecommons.org/licenses/by/4.0/>).

## 1. Introduction

With the substantial growth in global mobile data traffic, it is projected to reach 607 Exabytes (EBs) per month by 2025 [1]. On average, each user is expected to generate about 39 EBs of data traffic, with nearly 70% of users utilizing mobile devices and networks [2]. Despite the significant improvement in capacity, with fifth-generation (5G) wireless networks boasting at least a 1000-fold increase compared to their predecessors [3], the data rates and energy efficiency they offer remain insufficient to meet the evolving demands and ensure the sustainable development of 5G and 6G communications [4]. Consequently, designing wireless communication systems with a lower energy consumption and higher data rates has emerged as one of the most formidable challenges in current network design [5].

The introduction of massive MIMO technology in wireless networks has significantly enhanced the system spectrum and energy efficiency [6], positioning it as a pivotal technology for advancing fifth-generation (5G) mobile communication networks [7]. However, traditional cellular-based massive MIMO networks [8] face challenges in providing uniform coverage, with inter-cell interference emerging as a major bottleneck hindering system capacity improvements. Addressing this issue, proposed cell-free (CF) massive MIMO systems offer substantial enhancements in spectral efficiency (SE) and coverage uniformity [9]. Their core concept involves deploying numerous cost-effective, distributed access points (APs) to collaboratively serve users [10], effectively mitigating inter-cell interference. Previous research endeavors have primarily been aimed at enhancing the overall performance within coverage areas, focusing on metrics such as the sum rate or energy efficiency.

For instance, Trang C. Mai et al. [11] investigated maximum–minimum fair power control for CF massive MIMO systems to bolster the system’s SE.

However, in real-world scenarios, the capacity increase achieved by deploying numerous access points (APs) in cell-free (CF) massive MIMO systems comes at the expense of elevated energy consumption [12]. Indu L. Shakya et al. [13] introduced a novel approach called joint AP selection and interference cancellation (JAPSIC) to relocate a multitude of distributed APs closer to mobile users. Jionghui Wang et al. [14] formulated the problem of joint beamforming and AP–user association for millimeter-wave CF massive MIMO systems in the downlink, proposing an algorithm based on alternating average reflection to enhance the performance in terms of the minimum rate and total rate. Nonetheless, these approaches and algorithms offer only limited reductions in energy consumption. To achieve a lower energy consumption, the utilization of reconfigurable intelligent surfaces (RISs) in CF massive MIMO systems presents a promising solution [15]. RISs, comprising numerous passive and cost-effective components, can intelligently adjust the wireless propagation environment. Typically deployed on building exteriors or ceilings, RISs enable non-line-of-sight (NLoS) communication using environment sensing, covering network blind spots while consuming minimal power and conserving resources, thereby enhancing the system capacity [16]. Currently, energy-efficient CF massive MIMO systems have attracted significant research attention. For instance, Y. Zhang et al. [17] proposed a hybrid beamforming system to maximize the energy efficiency (EE) of RIS-assisted CF massive MIMO systems, investigating the influence of transmit power, RIS count, and RIS size on EE. M. Alonzo et al. [18] devised an uplink coordinated transmission strategy leveraging RIS backscattering, considering uplink weighted signal-to-residual ratio (SR) in RIS-assisted CF systems.

Although RIS-assisted communication in CF massive MIMO systems reduces some energy consumption, the overall energy consumption increases when all access points (APs) serve users in low-load states. Lan M et al. [19] proposed a novel framework for RIS-assisted CF massive MIMO systems to address this issue. This framework involves deploying additional active APs near the passive RIS and devising a user-centric AP selection strategy. However, this system’s deployment requires a large number of RISs, and the circuit losses of the RIS itself impose a significant burden on the system. To address this, we introduce RIS switching and AP sleep strategies in RIS-assisted CF massive MIMO systems, focusing on maximizing energy efficiency in the downlink. The primary contributions are outlined as follows:

1. An RIS-assisted CF massive MIMO system is considered, and an RIS switching strategy and an AP sleep strategy are introduced to reduce the system’s energy consumption.
2. A complex optimization problem involving four variables, namely the RIS phase shift, beamforming vector, AP, and RIS integer variables, is formulated to maximize the system’s energy efficiency.
3. An alternating optimization algorithm based on block gradient descent is proposed. The nonconvex optimization problem is initially decomposed into three sub-problems. In the optimization problem for RIS phase shifts, Lagrangian duality and the fractional programming method are sequentially applied, and the successive convex approximation (SCA) algorithm is utilized for problem resolution. For the beamforming vector and AP integer variable optimization problem, the variational programming method is employed to handle the integer variables, and the Dinkelbach algorithm and alternating direction method of multipliers (ADMM) algorithm are jointly utilized for problem resolution. The greedy algorithm is employed in the optimization problem for RIS switching. Finally, the optimization problem is converged through successive iterations of solving sub-problems.

The rest of this article is organized as follows. A system model of the RIS-assisted CF massive MIMO system is provided in Section 2. Subsequently, the formulation of the energy efficiency maximization problem is presented in Section 3, which outlines the algorithms for the joint beamforming vector, phase shift, AP sleep integer variable, and RIS



$\mathbf{G}_{r,l} \in N_r \times M$  and the channel matrix from RIS  $r$  to user  $k$  is  $\mathbf{h}_{r,k} \in N_r$ , where  $k = 1, \dots, K$  denotes the number of users and  $r = 1, \dots, R$  denotes the number of RISs. The channel of the system model was modeled as the direct communication link from the AP to the user and the RIS-assisted AP communication channel. The RIS-assisted AP communication channel is composed of the communication link  $\mathbf{G}_{r,l}$  from the AP to the RIS, the RIS phase shift matrix  $\Phi_r \in N_r \times N_r$  and the communication link  $\mathbf{h}_{r,k}$  from the RIS to the user.  $\Phi_r = \text{diag}(\phi_r)$  is the phase shift matrix of RIS, where  $\phi_r = [\phi_{r,1}, \phi_{r,2}, \dots, \phi_{r,N_r}]^T \in N_r$ ,  $\phi_{r,n} = \beta_n e^{j\theta_{rn}}$ ,  $\theta_{rn} \in [0, 2\pi]$ ,  $r \in \mathcal{R}$  and  $n \in \mathcal{N}_r = \{1, \dots, N_r\}$ . Let  $\theta_{rn}$  denote the phase shift of the  $n$ th reflecting element at the  $r$ th RIS.  $\beta_n \in \{0, 1\}$  represents the switching state of the  $n$ th reflecting element of a certain RIS, which is generally set to  $\beta_n = 1$  in order to maximize the signal reflection.

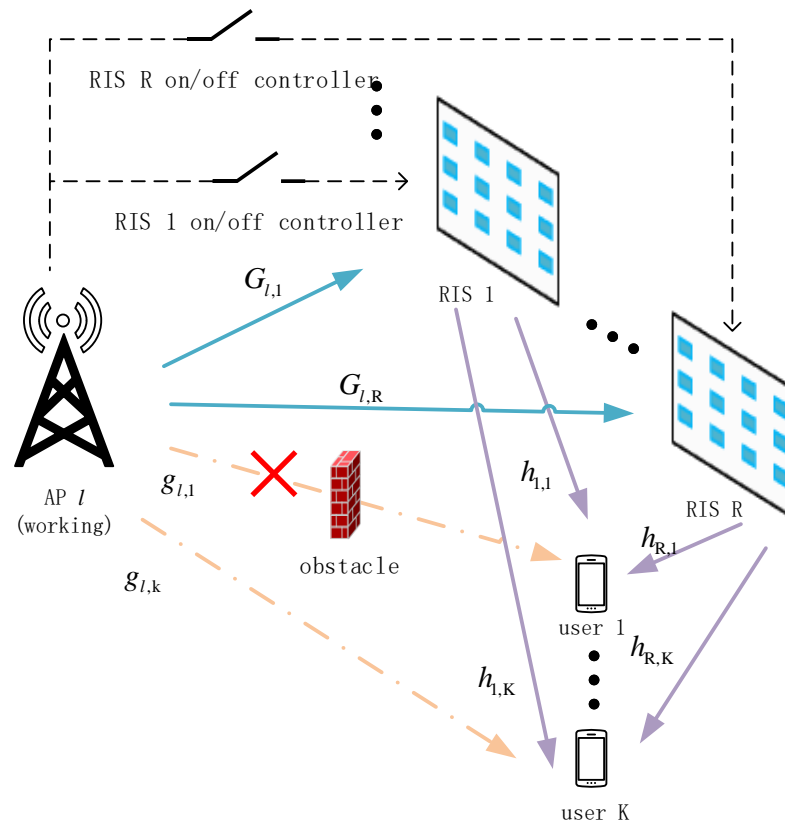


Figure 2. RIS-assisted CF massive MIMO system model.

2.2. Transmission Model

The signal transmitted at the AP  $l$  is modeled as follows

$$\mathbf{m}_l = \sum_{k=1}^K \mathbf{w}_{l,k} s_k, \tag{1}$$

where  $\mathbf{w}_{l,k}$  ( $k \in \mathcal{K}, l \in \mathcal{L}$ ) is the beamforming vector of the user  $k$  at the AP  $l$ .  $s_k$  is the signal value of the  $k$ th user and  $E\{|s_k|^2\} = 1, k = 1, 2, \dots, K$ .

The AP power consumption depends on power amplifier (PA) power dissipation, leakage power dissipation and chip power dissipation. Considering the transmission power of APs to users and their own circuit losses, accessing all APs is usually not energy efficient. To this end, a binary variable  $x_l \in \{0, 1\}$  is introduced in this article. Let  $x_l = 1$  denote that the AP is working and let  $x_l = 0$  denote that the AP is sleeping. In addition, another binary variable  $c_r \in \{0, 1\}$  is introduced, considering the loss of RIS itself. Let  $c_r = 1$  denote that the RIS is on and let  $c_r = 0$  denote that the RIS is off.

The signal received by the user  $k$  is as follows:

$$y_k = \sum_{l=1}^L \left( \sum_{r=1}^R x_l c_r \mathbf{h}_{r,k}^H \Phi_r \mathbf{G}_{r,l} + x_l \mathbf{g}_{l,k}^H \right) \mathbf{m}_l + n_k, \tag{2}$$

where  $\mathbf{g}_{l,k}$ ,  $\mathbf{h}_{r,k}$ , and  $\mathbf{G}_{r,l}$  denote the channel from the  $l$ th AP to the  $k$ th user, from the  $r$ th RIS to the  $k$ th user, and from the  $l$ th AP to the  $r$ th RIS, respectively. In addition,  $n_k \sim \mathcal{CN}(0, \delta^2)$  is the additive white Gaussian noise (AWGN) of user  $k$ .  $\Phi_r$  is the reflection matrix, which can also be called the passive beamformer; it contains the reflection amplitude and the reflection phase formed by  $N_r$  reflection elements and is controlled by the RIS deployed near the AP  $l$ .  $\Phi_r$  can be expressed as follows

$$\Phi_r = \text{diag} \left( A(\angle \Gamma_1^r) e^{j\angle \Gamma_1^r}, A(\angle \Gamma_2^r) e^{j\angle \Gamma_2^r}, \dots, A(\angle \Gamma_{N_r}^r) \times e^{j\angle \Gamma_{N_r}^r} \right), \tag{3}$$

where  $A(\angle \Gamma_n^r)$  denotes the reflection amplitude at the reflection element  $n$  of the RIS  $r$ , and  $\angle \Gamma_n^r$  denotes the phase at the reflection element  $n$  of the RIS  $r$ . In this article, to maximize the signal reflection, the reflection amplitude  $A(\angle \Gamma_n^r)$  is set to 1 and  $\theta_{rn}$  is used to denote the phase  $\angle \Gamma_n^r$ .  $\Phi_r$  can be rewritten as follows:

$$\Phi_r = \text{diag} \left( e^{j\theta_{r1}}, e^{j\theta_{r2}}, \dots, e^{j\theta_{rN_r}} \right), \tag{4}$$

To facilitate SINR calculation, set  $\tilde{\mathbf{H}}_{l,k} \triangleq \sum_{r=1}^R c_r \mathbf{h}_{r,k}^H \Phi_r \mathbf{G}_{r,l} + \mathbf{g}_{l,k}^H$ , where  $c_r \mathbf{h}_{r,k}^H \Phi_r \mathbf{G}_{r,l} = c_r \phi_r^H \text{diag} \left( \mathbf{h}_{r,k}^H \right) \mathbf{G}_{r,l}$ . Then, the received signal at the user  $k$  can be converted to:

$$y_k = \sum_{l=1}^L x_l \tilde{\mathbf{H}}_{l,k} \mathbf{w}_{l,k} s_k + \sum_{l=1}^L \sum_{j=1, j \neq k}^K x_l \tilde{\mathbf{H}}_{l,k} \mathbf{w}_{l,j} s_j + n_k, \tag{5}$$

Based on Equations (1) and (5), the signal to interference plus noise ratio (SINR) of user  $k$  is defined as follows:

$$\text{SINR}_k = \frac{\sum_{l=1}^L |x_l \tilde{\mathbf{H}}_{l,k} \mathbf{w}_{l,k}|^2}{\sum_{l=1}^L \sum_{j=1, j \neq k}^K |x_l \tilde{\mathbf{H}}_{l,k} \mathbf{w}_{l,j}|^2 + \delta^2}, \tag{6}$$

The total power constraint at the AP  $l$  is as follows:

$$\sum_{l=1}^L \sum_{k=1}^K x_l \mathbf{w}_{l,k}^H \mathbf{w}_{l,k} \leq P_{\max}, \tag{7}$$

where  $P_{\max}$  is the maximum transmit power of the AP. When the AP  $l$  transmits a signal to the user  $k$  through the maximum transmit power,  $\text{SINR}_k$  reaches its maximum value;

that is, the two conditions  $\mathbf{w}_{l,k}^H \mathbf{w}_{l,k} \leq P_{\max}$  and  $\text{SINR}_k^{\max} = \frac{\sum_{l=1}^L |x_l \tilde{\mathbf{H}}_{l,k}|^2 P_{\max}}{\delta^2}$  are satisfied. Therefore, the range of  $\text{SINR}_k$  is  $0 \leq \text{SINR}_k \leq \text{SINR}_k^{\max}$ .

In addition, the total user rate can be defined as follows:

$$R_t = B \sum_{k=1}^K \log_2(1 + \text{SINR}_k). \tag{8}$$

where  $B$  denotes the bandwidth of the channel.

### 2.3. Power Consumption Model

The total power consumption of the system is divided into four parts, which are the transmit power from the AP to the user, the circuit loss of the AP, the power consumption

of the backhaul network between the CPU and the AP, the circuit loss of the user, and the circuit loss of the RIS. The power consumption from AP  $l$  to user  $k$  is defined as follows:

$$P_{l,k} = \mu p_k + x_l P_l + P_k + c_r P_{RIS}, \tag{9}$$

where  $\mu = \nu^{-1}$  ( $\nu$  is the power amplification factor of the AP) and  $P_l$  and  $P_k$  are the circuit losses of AP  $l$  and user  $k$ , respectively. Let  $P_{RIS} = N_r P_r$  denote the total power consumption of the RIS  $r$ , where  $P_r$  denotes the power consumption of each reflective element in the RIS  $r$ . Since the numbers of users and APs are fixed,  $P_A$  is constant. Therefore, the total power consumption can be rewritten as follows:

$$P_t = \sum_{l=1}^L \sum_{k=1}^K \mu x_l \mathbf{w}_{l,k}^H \mathbf{w}_{l,k} + \sum_{l=1}^L x_l P_l + \sum_{k=1}^K P_k + \sum_{r=1}^R c_r N_r P_r + P_A. \tag{10}$$

where  $\mu x_l \mathbf{w}_{l,k}^H \mathbf{w}_{l,k}$  is the power consumption of the AP.

### 3. Problem Modeling and Solving

#### 3.1. Problem Modeling

Based on the above system model, the goal of this article is to jointly optimize the reflection coefficient matrix, beamforming vector, RIS switching variables, and AP integer variables to maximize the energy efficiency under the total power constraint. The EE is defined as the ratio of the total rate (bps) to the total power consumption (joules) of the RIS-assisted communication system, that is,  $EE = R_t/P_t$ . According to Equations (8) and (10), the EE can be expressed as follows:

$$EE = \frac{B \sum_{k=1}^K \log_2(1 + SINR_k)}{\sum_{l=1}^L \sum_{k=1}^K \mu x_l \mathbf{w}_{l,k}^H \mathbf{w}_{l,k} + \sum_{l=1}^L x_l P_l + \sum_{k=1}^K P_k + \sum_{r=1}^R c_r N_r P_r}, \tag{11}$$

The objective problem is transformed into EE maximization.

$$\mathcal{P}_0 : \max_{\mathbf{w}, \theta, \mathbf{x}, \mathbf{c}} EE, \tag{12}$$

such that

$$\sum_{l=1}^L \sum_{k=1}^K x_l \mathbf{w}_{l,k}^H \mathbf{w}_{l,k} \leq LP_{\max}, \tag{13}$$

$$\theta_{rn} \in [0, 2\pi], \forall r, n, \tag{14}$$

$$x_l \in \{0, 1\}, \forall l, \tag{15}$$

$$c_r \in \{0, 1\}, \forall r. \tag{16}$$

where  $\mathbf{w} = [\mathbf{w}_{1,1}, \dots, \mathbf{w}_{1,K}, \dots, \mathbf{w}_{L,1}, \dots, \mathbf{w}_{L,K}]$ ,  $\boldsymbol{\theta} = [\theta_{r1}, \dots, \theta_{rN_R}]^T$ ,  $\mathbf{x} = [x_1, \dots, x_L]^T$ ,  $P_{\max}$  is the maximum transmit power of the AP. Equation (13) represents the total power constraint, Equation (14) represents the RIS phase shift constraint, and Equations (15) and (16) are integer variable constraints. Due to the integer constraints (15) and (16), non-convex constraints, and coupled variables, the optimization problem  $\mathcal{P}$  is a mixed-integer nonlinear programming (MINLP) problem that cannot be solved directly and needs to be further transformed and processed.

#### 3.2. Problem Solving

Since the optimization problem includes coupling, inequality constraints, integer variables, etc., it is difficult to solve problem (12) directly. In order to maximize the energy efficiency of the system, a low-complexity iterative algorithm is proposed to find the

suboptimal solution, which alternately optimizes the phase shift of the RIS, the switch integer variables of the RIS, the beamforming vector, and the AP integer variables.

### 3.2.1. Optimization of RIS Components $\Phi$

Given the beamforming vector  $\mathbf{w}$ , AP integer variables  $\mathbf{x}$ , and RIS switch variables  $\mathbf{c}$ , the total power consumption of the system is unchanged, and the energy efficiency maximization is equivalent to the sum rate maximization. Problem (12) can be written as follows:

$$\mathcal{P}_1 : \max_{\Phi} R_t, \tag{17}$$

By setting  $f_0(\mathbf{w}, \Phi, x, c) = B \sum_{k=1}^K \log_2(1 + SINR_k)$ , through the Lagrangian dual transformation [20],  $f_0$  can be transformed into:

$$f_r(\mathbf{w}, \Phi, \mathbf{x}, \mathbf{c}, \gamma) = B \sum_{k=1}^K \log_2(1 + \gamma_k) - B \sum_{k=1}^K \frac{1}{\ln 2} \gamma_k + B \sum_{k=1}^K \frac{(1 + \gamma_k) \sum_{l=1}^L |x_l \bar{\mathbf{H}}_{l,k} \mathbf{w}_{l,k}|^2}{\ln 2 \left( \sum_{l=1}^L \sum_{j=1}^K |x_l \bar{\mathbf{H}}_{l,k} \mathbf{w}_{l,j}|^2 + \delta^2 \right)}, \tag{18}$$

$\gamma_k$  is the introduced auxiliary variable and  $\gamma$  denotes the set of such auxiliary variables. Since constraint (14) does not contain auxiliary variables  $\gamma$ , the optimal solution  $\gamma$  can be solved by  $\partial f_r / \partial \gamma_k = 0$ . The expression is as follows:

$$\gamma_k^* = \frac{\sum_{l=1}^L |x_l \bar{\mathbf{H}}_{l,k} \mathbf{w}_{l,k}|^2}{\sum_{l=1}^L \sum_{j=1, j \neq k}^K |x_l \bar{\mathbf{H}}_{l,k} \mathbf{w}_{l,j}|^2 + \delta^2}, \tag{19}$$

Considering that the fractional sum form of the last term in Equation (18) still makes the objective function non-convex, the fractional programming (FP) method [21] is introduced to further process it. By introducing the auxiliary variable  $y_{l,k}$  into the ratio term,  $f_r(\mathbf{w}, \Phi, \mathbf{x}, \mathbf{c}, \gamma)$  can be transformed into  $f_q(\mathbf{w}, \Phi, \mathbf{x}, \mathbf{c}, \gamma, \mathbf{y})$ .

$$f_q(\mathbf{w}, \Phi, x, c, \gamma, \mathbf{y}) = B \sum_{k=1}^K [\log_2(1 + \gamma_k) - \frac{1}{\ln 2} \gamma_k + \frac{1 + \gamma_k}{\ln 2} \sum_{l=1}^L \{2 \operatorname{Re}\{y_{l,k}^H \bar{x} \bar{\mathbf{H}}_{l,k} \mathbf{w}_{l,k}\} - |y_{l,k}|^2 (\sum_{i=1}^L \sum_{j=1}^K |x_i \bar{\mathbf{H}}_{i,k} \mathbf{w}_{i,j}|^2 + \delta^2)\}], \tag{20}$$

where  $\mathbf{y}$  denotes the set of auxiliary variables  $y_{l,k}$ . Similarly, the optimal solution  $\mathbf{y}$  is expressed as follows:

$$y_{l,k}^* = \frac{x_l \bar{\mathbf{H}}_{l,k} \mathbf{w}_{l,k}}{\sum_{i=1}^L \sum_{j=1}^K |x_i \bar{\mathbf{H}}_{i,k} \mathbf{w}_{i,j}|^2 + \delta^2}, \tag{21}$$

The problem  $\mathcal{P}_1$  can be rewritten as follows:

$$\mathcal{P}_2 : \max_{\Phi} f_q(\Phi, \mathbf{w}^j, \mathbf{x}^j, \mathbf{c}^j, \gamma^{j+1}, \mathbf{y}^{j+1}), \tag{22}$$

Because  $\bar{\mathbf{H}}_{l,k} = \sum_{r=1}^R c_r \phi_r^H \operatorname{diag}(\mathbf{h}_{r,k}^H) \mathbf{G}_{r,l} + \mathbf{g}_{l,k}^H$ , problem (22) is transformed as follows:

$$\mathcal{P}_3 : \max_{\Phi} f_q(\Phi, \mathbf{w}^j, \mathbf{x}^j, \mathbf{c}^j, \gamma^{j+1}, \mathbf{y}^{j+1}), \tag{23}$$

where  $\boldsymbol{\phi}_r = [\phi_{r,1}, \phi_{r,2}, \dots, \phi_{r,N_r}]^T \in N_r$ ,  $\phi_{r,n} = e^{j\theta_{rn}}$ . It follows that  $\mathcal{P}_3$  is still non-convex and can be approximated by the SCA algorithm.  $\phi_{r,n}$  can be approximated by  $e^{j\theta_m^{(i-1)}} + je^{j\theta_m^{(i-1)}}(\theta_{rn} - \theta_{rn}^{(i-1)})$ . The problem  $\mathcal{P}_3$  is rewritten as

$$\mathcal{P}_4 : \max_{\boldsymbol{\theta}} f_q(\boldsymbol{\theta}, \mathbf{w}^j, \mathbf{x}^j, \mathbf{c}^j, \gamma^{j+1}, \mathbf{y}^{j+1}). \tag{24}$$

This problem is a typical convex optimization problem, and there is no variable coupling, which can be solved directly by the cvx solver.

### 3.2.2. Optimization of Beamforming Vectors $\mathbf{w}$ and AP Integer Variables $\mathbf{x}$

Given the phase shift of the RIS  $\boldsymbol{\theta}$  and the RIS switch variables  $\mathbf{c}$ , problem (12) is transformed into:

$$\mathcal{P}_5 : \max_{\mathbf{w}, \mathbf{x}, \boldsymbol{\zeta}} \frac{B \sum_{k=1}^K \log_2(1 + \zeta_k)}{P_t}, \tag{25}$$

such that

$$\zeta_k \leq \frac{\sum_{l=1}^L |x_l \bar{\mathbf{H}}_{l,k} \mathbf{w}_{l,k}|^2}{\sum_{l=1}^L \sum_{j=1, j \neq k}^K |x_l \bar{\mathbf{H}}_{l,k} \mathbf{w}_{l,j}|^2 + \delta^2}, \forall k, \tag{26}$$

(13), (15)

where  $\boldsymbol{\zeta} = [\zeta_1, \dots, \zeta_K]^T$  and  $\zeta$  is a slack variable that ensures that constraint (26) is always equal to the optimal solution. Due to the integer constraint (15),  $\mathcal{P}_5$  is still a non-convex problem. To this end, the variational programming method [22] is used in this article to deal with the variable  $\mathbf{x}$ , and auxiliary variables  $\mathbf{d}$  are introduced to ensure equivalence. Equation (15) is transformed into

$$0 \leq x_l \leq 1, \forall l, \tag{27}$$

$$\|2\mathbf{d} - \mathbf{1}\|_2^2 \leq L, \tag{28}$$

$$(2\mathbf{x} - \mathbf{1})^T (2\mathbf{d} - \mathbf{1}) = L, \tag{29}$$

To deal with the coupling problem of  $\mathbf{w}$  and  $\mathbf{x}$  in problem (25) and constraints (13) and (26), according to the potential connection between the beamforming vector  $\mathbf{w}$ , the SINR  $\gamma_k$  and the integer variable  $\mathbf{x}$  of the AP, the non-working APs should not transmit signals to prevent resource waste. So, we introduce an extra constraint:

$$\|\mathbf{w}_{l,k}\|^2 \leq x_l P_{\max}, \tag{30}$$

$$x_l (\sum \gamma_k - c) \geq 0, \tag{31}$$

Equation (30) ensures that when  $x_l = 0$ ,  $\mathbf{w}_{l,k} = 0$ . In Equation (31),  $c$  is a small positive number, which guarantees that when  $\sum \gamma_k = 0$ ,  $x_l = 0$ . At this point, the variable  $\mathbf{x}$  coupled in the target problem (25) and constraints (13) and (26) can be omitted.

To deal with the non-convexity of constraint (26), slack variable  $\alpha_{l,k} > 0$  is introduced and constraint (26) is reformulated as follows:

$$\sum_{l=1}^L |\bar{\mathbf{H}}_{l,k} \mathbf{w}_{l,k}|^2 \geq \zeta_k \sum_{l=1}^L \alpha_{l,k}, \forall k, \tag{32}$$

and

$$\sum_{l=1}^L \sum_{j=1, j \neq k}^K |\bar{\mathbf{H}}_{l,k} \mathbf{w}_{l,j}|^2 + \delta^2 \leq \sum_{l=1}^L \alpha_{l,k}, \forall k, \tag{33}$$

In the general case,  $\bar{\mathbf{H}}_{l,k}\mathbf{w}_{l,k}$  in constraint (32) can be made real by any rotation of  $\mathbf{w}_{l,k}$ . Thus, constraint (32) can be transformed into  $\sum_{l=1}^L \mathcal{R}(\bar{\mathbf{H}}_{l,k}\mathbf{w}_{l,k}) \geq \sum_{l=1}^L \sqrt{\zeta_k \alpha_{l,k}}$  by relaxation. Taking the first-order Taylor expansion of the concave function  $\sqrt{\zeta_k \alpha_{l,k}}$ , constraint (32) becomes:

$$\sum_{l=1}^L \mathcal{R}(x_l \bar{\mathbf{H}}_{l,k}\mathbf{w}_{l,k}) \geq \sum_{l=1}^L \left( \sqrt{\zeta_k^{(i-1)} \alpha_{l,k}^{(i-1)}} + \frac{1}{2} \sqrt{\frac{\zeta_k^{(i-1)}}{\alpha_{l,k}^{(i-1)}}} (\alpha_{l,k} - \alpha_{l,k}^{(i-1)}) + \frac{1}{2} \sqrt{\frac{\alpha_{l,k}^{(i-1)}}{\zeta_k^{(i-1)}}} (\zeta_k - \zeta_k^{(i-1)}) \right) \tag{34}$$

After the above processing, the objective function has been transformed into the standard form of a concave function divided by a convex function, but there is still a variable coupling problem in constraint (29), so the objective function cannot be directly solved by the Dinkelbach algorithm. Therefore, the Dinkelbach method, the alternating direction method of multipliers [21] and the block coordinate update fusion algorithm are proposed to decompose the coupling problem into multiple sub-problems and solve them, respectively. Firstly, the Dinkelbach algorithm [23] was used to transform the objective function as follows:

$$\mathcal{P}_6 : \max_{\mathbf{w}, \mathbf{x}, \mathbf{d}, \zeta, \alpha} B \sum_{k=1}^K \log_2(1 + \zeta_k) - \chi^{(i-1)} \left( \sum_{l=1}^L \sum_{k=1}^K \mu \mathbf{w}_{l,k}^H \mathbf{w}_{l,k} + \sum_{l=1}^L x_l P_l + \sum_{k=1}^K P_k + \sum_{r=1}^R c_r N_r P_r \right) \tag{35}$$

such that

$$\sum_{l=1}^L \sum_{k=1}^K \mathbf{w}_{l,k}^H \mathbf{w}_{l,k} \leq LP_{\max}, \tag{36}$$

$$\alpha_{l,k} > 0, \tag{37}$$

$$(27) - (31), (33) - (34)$$

where

$$\chi^{(i)} = \frac{B \sum_{k=1}^K \log_2(1 + \zeta_k^i)}{P_t^i}, \tag{38}$$

In view of the coupling of  $\mathbf{x}$  and  $\mathbf{d}$  in constraint condition (29), the ADMM algorithm is introduced to update variables alternately by combining dual decomposition and the augmented Lagrangian method. Let  $g(\mathbf{x}, \mathbf{d}) = L - (2\mathbf{x} - \mathbf{1})^T(2\mathbf{d} - \mathbf{1})$ , introduce the Lagrange multiplier  $\zeta$  and penalty parameter  $\rho > 0$ , and then the augmented Lagrange equation is as follows:

$$\mathcal{L}_A(\mathbf{w}, \mathbf{x}, \mathbf{d}, \zeta, \alpha; \xi) = B \sum_{k=1}^K \log_2(1 + \zeta_k) - \chi^{(i-1)} P_t - \zeta g(\mathbf{x}, \mathbf{d}) - \frac{\rho}{2} (g(\mathbf{x}, \mathbf{d}))^2, \tag{39}$$

Problem (39) is treated as a traditional ADMM problem and solved by iteration. The algorithm for each iteration is as follows:

1. Update the variable  $\mathbf{d}$

$$\mathbf{d}^{i+1} = \arg \max_{\mathbf{d}} \mathcal{L}_A(\mathbf{w}^i, x^i, d, \zeta^i, \alpha^i; \xi^i), \tag{40}$$

such that

$$(28)$$

where the superscript  $(i + 1)$  represents the  $(i + 1)$ th iteration. The Lagrange multiplier method is used to obtain Equation (41), and  $b$  is the Lagrange multiplier of Equation (28). The optimal solution of  $b$  and  $\mathbf{d}$  can be found by a bisection line search.

$$\mathbf{d} = \frac{1}{2} + \frac{(\zeta^i + \rho L)(2\mathbf{x}^i - \mathbf{1})}{4b\mathbf{1} + 2\rho(2\mathbf{x}^i - \mathbf{1})(2\mathbf{x}^i - \mathbf{1})^T}, \quad (41)$$

2. Update the remaining variables except the Lagrange multiplier. The objective function is updated as follows:

$$\mathcal{P}_7 : \max_{\mathbf{w}, \mathbf{x}, \zeta, \alpha} \mathcal{L}_A(\mathbf{w}, \mathbf{x}, \mathbf{d}^{i+1}, \zeta, \alpha; \xi), \quad (42)$$

such that

$$(27) - (28), (30) - (31), (33) - (34)$$

The problem can be solved directly by the cvx solver in MATLAB.

3. Update the Lagrange multiplier. Lagrange multipliers are obtained by a subgradient search:

$$\zeta^{i+1} = \zeta^i + \rho g(\mathbf{x}^{i+1}, \mathbf{d}^{i+1}) \quad (43)$$

4. Update the Dinkelbach auxiliary variable. Update Equation (38) until convergence. The specific algorithm for this subsection is shown in Algorithm 1.

---

**Algorithm 1** Joint Algorithm for Beam Coordination and AP Sleep Based on Dinkelbach and ADMM

---

- 1: Initialize channel model parameters and channel vectors. Set iteration number  $i = 1$  and maximum number of iterations.
  - 2: **repeat**
  - 3:     Updating the variable  $\mathbf{d}$  by Equation (41),
  - 4:     Updating the remaining variables except the Lagrange multiplier by Equation (42),
  - 5:     Updating the Lagrange multiplier by Equation (43),
  - 6:     Updating the Dinkelbach auxiliary variable by Equation (38),
  - 7:      $i = i + 1$ ,
  - 8: **until** the objective value converges or the end of the iteration.
  - 9: Output AP integer variables, beamforming vectors.
- 

### 3.2.3. Optimization of the RIS Switch Variable $\mathbf{c}$

The remaining variables except  $\mathbf{c}$  are fixed and solved via a greedy algorithm. If the objective value (12) can be improved and the new solution is feasible, try to close an RIS. If the new solution is feasible, try to close an RIS for loop. If the new solution is not feasible, record the objective value as 0. When closing any RIS does not improve the energy efficiency, terminate the loop and output.

### 3.2.4. Complexity Analysis

The block gradient-descent based alternating optimization algorithm proposed in this article is detailed in Algorithm 2. From Algorithm 2, the complexity of solving problem (11) is mainly the complexity of solving the phase optimization problem in (17), the joint beamforming and AP integer variable optimization problem (25), and the RIS switching variable optimization problem.

For the phase optimization problem of RISs, we adopt the SCA algorithm; then, the total complexity of solving problem (17) is  $\mathcal{O}(T^{3.5}K^{3.5} \log_2(1/\epsilon_1))$  [24,25], where  $\epsilon_1$  is the accuracy of the SCA algorithm in solving problem (17). Similarly, the computational complexity of solving problem (25) via Algorithm 1 is mainly caused by problem (42), whose total complexity is  $\mathcal{O}(ZT^{3.5}K^{3.5})$ , where  $Z$  is the number of iterations of Dinkelbach's algorithm. The total complexity of the RIS switching optimization problem based on the greedy algorithm is  $\mathcal{O}(A^2RN_rB)$ , where  $A^2$  denotes the total number of iterations of the greedy algorithm and  $B$  is the number of RISs in the working state.

Therefore, the total complexity of Algorithm 2 to solve the problem (11) is  $\mathcal{O}(sT^{3.5}K^{3.5} \log_2(1/\epsilon_1) + sZT^{3.5}K^{3.5} + sA^2RN_rB)$ , where  $s$  is the number of iterations of Algorithm 2. Algorithm 2 proposed in this article has a lower complexity than the algorithm in [26].

---

**Algorithm 2** Alternating optimization algorithm based on block gradient descent

---

- 1: Initialize channel model parameters and channel vectors. Set iteration number  $k = 1$  and maximum number of iterations.
  - 2: **repeat**
  - 3:     Updating the variable  $\Phi$  by SCA algorithm,
  - 4:     Updating beamforming vectors  $\mathbf{w}$  and AP integer variables  $\mathbf{x}$  by Algorithm 1,
  - 5:     Updating RIS switch variable  $\mathbf{c}$  by greedy algorithm,
  - 6: **until** the objective value converges or the end of the iteration.
  - 7:      $k = k + 1$ ,
  - 8: Output AP integer variables, beamforming vectors, RIS phase shift, RIS integer variable.
- 

#### 4. Simulation Results and Analysis

In this article, the performance of the proposed RIS-assisted AP access scheme for CF massive MIMO systems is simulated and analyzed. The number of APs, the number of RISs and the number of users are set to 8, 16 and 3, respectively. The deployment of APs, RISs, and users follows a Poisson distribution, and the other parameters are shown in Table 1.

**Table 1.** Simulation parameters.

Parameter	Value
AP circuit power $P_l$	30 dBm
Maximum transmission power of AP $P_{\max}$	26 dBm
User circuit power $P_k$	10 dBm
RIS circuit Power $P_{RIS}$	10 dBm
Total bandwidth	20 MHz
Center frequency	2.4 GHz
Noise power spectral density	−174 dBm/Hz
Number of AP antennas	4
The number of reflective elements of the RISs	64

Figure 3 compares the iterative algorithm with the AP fully connected scheme, the RIS fully connected scheme, the AP and RIS fully connected scheme, and the no RIS scheme. The proposed scheme has a higher EE, the values of which were increased by 3%, 26%, 35% and 63% respectively, compared to the other programs. It can be clearly seen that the scheme proposed in this article exhibits a nearly two-fold improvement compared to the RIS-less scheme in terms of EE. The effectiveness of RISs in CF mMIMO systems can be demonstrated when compared to the AP and RIS fully connected scheme. The AP sleep strategy has more impact on the EE of the system than the RIS switching strategy. This verifies the effectiveness of the proposed algorithm in solving the EE of an RIS-assisted CF massive MIMO system.

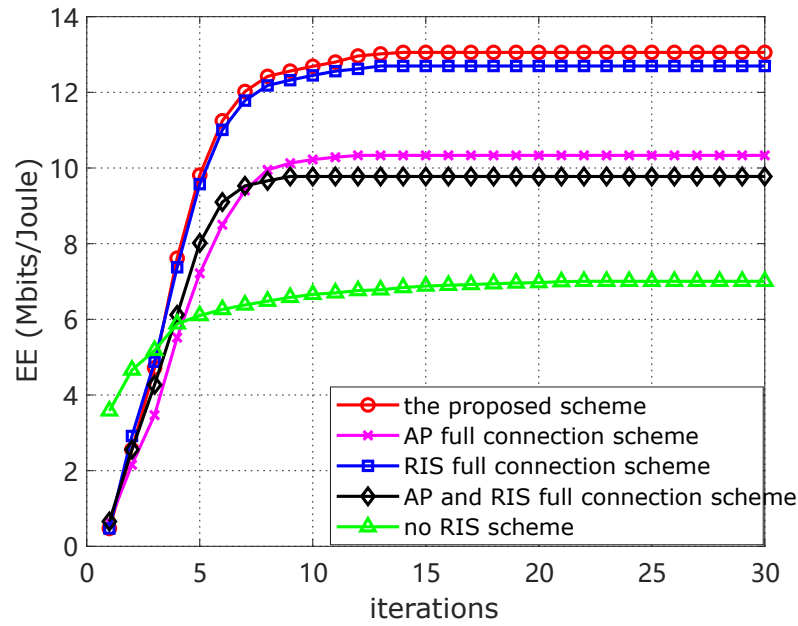


Figure 3. EE versus the number of iterations.

Figure 4 illustrates the EE variation of each scheme when changing the number of RIS elements. Except for the no RIS scheme, when the number of RIS elements is in the range of 58 to 68, the system’s EE increases with the number of RIS elements. First of all, for the no RIS scheme, the change in the number of RIS components does not have any effect on EE. Therefore, there is almost no change in the no RIS scheme. Although RISs require less power consumption and their impact on the EE is lower, the scheme proposed in this article considers the switching of RISs and still has about a 3% improvement in EE compared to the RIS fully connected scheme. It is obvious that the proposed scheme is more energy efficient compared to other schemes.

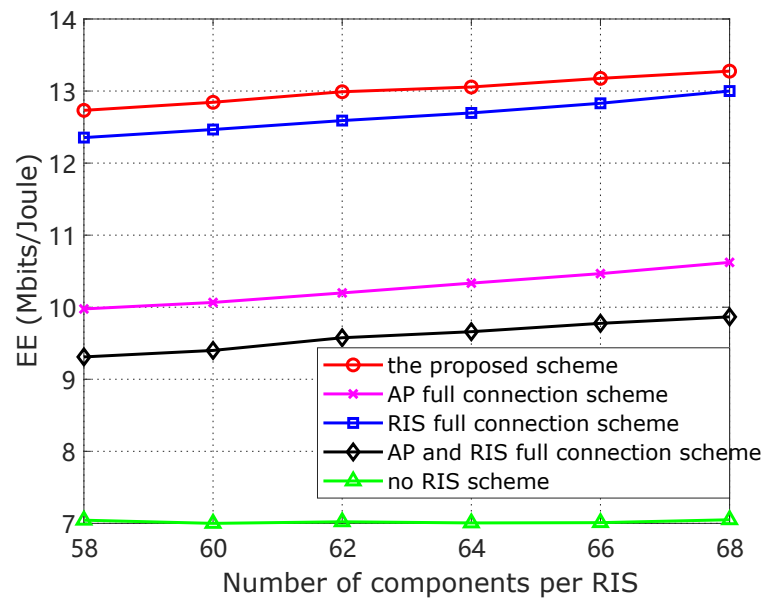


Figure 4. Relationship between EE and the number of RIS elements.

Figure 5 depicts the energy efficiency of each scheme for different AP maximum transmit powers. Overall, the trends in Figure 5 are similar to those in Figure 4. The biggest difference is that the AP transmission power has an effect on the EE value of the no RIS scheme. When the AP transmission power increases, the EE values of all schemes increase

essentially linearly. The EE values of the proposed scheme with respect to the no RIS scheme are roughly twice as high as those with respect to the AP and RIS fully connected schemes. The EE increases linearly with the transmit power, which verifies the effectiveness of the proposed scheme.

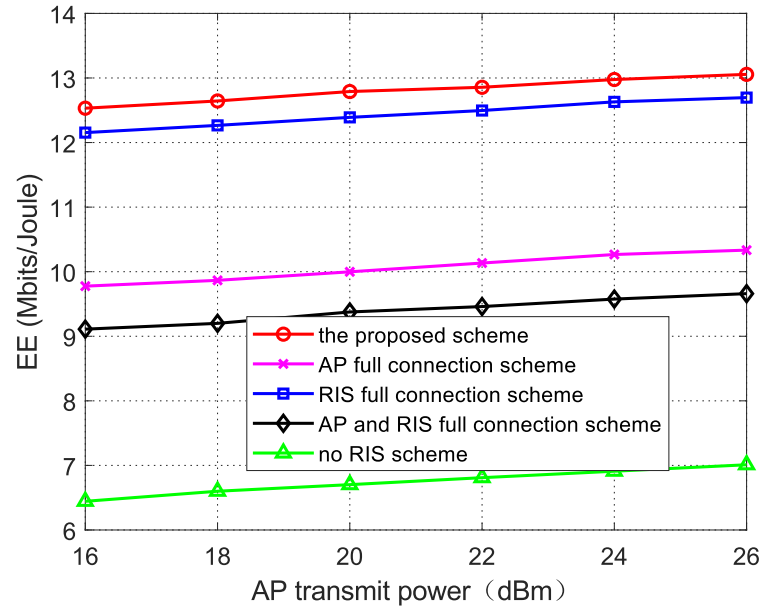


Figure 5. Relationship between EE and AP transmit power.

Figure 6 considers the relationship between the number of elements of the RIS and the EE at transmission powers of 16, 20, and 24 dBm, respectively. From the figure, it can be seen that in the proposed scheme, the EE value is proportional to the transmission power and the number of RIS elements. This is due to the low power consumption of RISs and the introduction of additional reflective elements. The increase in the system’s energy consumption is small, which leads to the high energy consumption of the system. This indicates that an RIS with a higher number of deployed elements is more energy efficient.

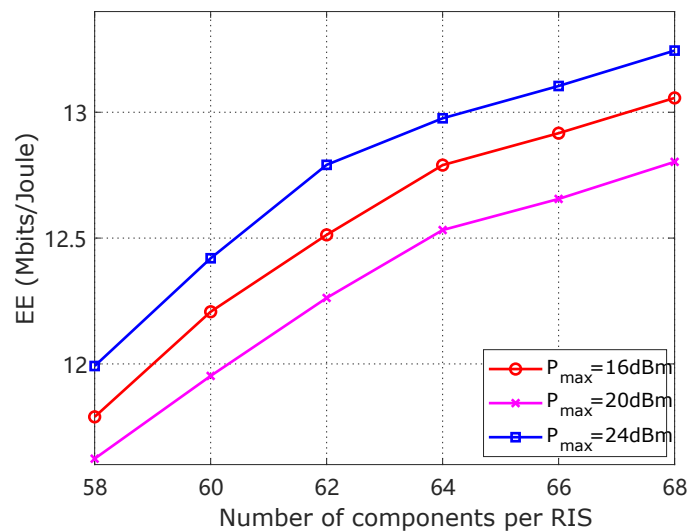


Figure 6. Relationship between EE and the number of RIS elements for three different AP transmission powers.

## 5. Conclusions and Outlook

In an effort to mitigate the increased power consumption of RIS-assisted CF massive MIMO systems, this study introduces both an AP sleep strategy and an RIS switching strategy. We present an iterative algorithm that jointly optimizes the RIS phase shift, beamforming vector, and the integer vectors of APs and RIS to maximize the EE, while adhering to constraints on the AP power, the RIS phase, and integer variables. The simulation results demonstrate the superior performance of the proposed joint iterative algorithm. Additionally, the implementation of RIS switching control and an AP sleep strategy is shown to enhance the EE of RIS-assisted CF massive MIMO systems. The EE values are improved by 35% and 63% compared to the two scenarios without considering the dormancy strategy and without considering RISs, respectively.

In conjunction with the research work in this article on the energy efficiency of RIS-assisted CF mMIMO systems, we will consider the application of millimeter waves in this system in our future work. Millimeter wave technology can lead to large bandwidths at high data rates and an increased system capacity, thus improving system performance. Effective utilization of RISs in millimeter-wave-based CF-mMIMO systems, RIS deployment planning, etc., pose challenges in terms of cost and practical implementation.

**Author Contributions:** Conceptualization, W.W.; methodology, W.W.; software, W.W.; validation, W.W. and J.S.; formal analysis, W.W.; writing—review and editing, W.W.; visualization, J.S.; supervision, J.Z. and W.W. All authors have read and agreed to the published version of the manuscript.

**Funding:** This research received no external funding.

**Data Availability Statement:** Data are contained with the article.

**Conflicts of Interest:** The author declares no conflicts of interest.

## References

1. Chettri, L.; Bera, R. A comprehensive survey on Internet of Things (IoT) toward 5G wireless systems. *IEEE Internet Things J.* **2019**, *7*, 16–32. [[CrossRef](#)]
2. Hande, P.; Tinnakornsriruphap, P.; Damnjanovic, J.; Xu, H.; Mondet, M.; Lee, H.Y.; Sakhnini, I. Extended Reality over 5G—Standards Evolution. *IEEE J. Sel. Areas Commun.* **2023**, *41*, 1757–1771. [[CrossRef](#)]
3. Hong, I.P. Reviews Based on the Reconfigurable Intelligent Surface Technical Issues. *Electronics* **2023**, *12*, 4489. [[CrossRef](#)]
4. Zhao, D.; Wang, G.; Wang, J.; Zhou, Z. Reconfigurable Intelligent Surface-Assisted Millimeter Wave Networks: Cell Association and Coverage Analysis. *Electronics* **2023**, *12*, 4270. [[CrossRef](#)]
5. Ni, L.; Zhu, Y.; Guo, W. Controllable Multiple Active Reconfigurable Intelligent Surfaces Assisted Anti-Jamming Communication. *Electronics* **2023**, *12*, 3933. [[CrossRef](#)]
6. de Figueiredo, F.A.P. An Overview of Massive MIMO for 5G and 6G. *IEEE Lat. Am. Trans.* **2022**, *20*, 931–940. [[CrossRef](#)]
7. Qian, P.; Zhang, Y.; Yan, X.; Chen, Y.; Sun, Y. A Robust Scheme for RIS-Assisted UAV Secure Communication in IoT. *Electronics* **2023**, *12*, 2507. [[CrossRef](#)]
8. Albreem, M.A.; Al Habbash, A.H.; Abu-Hudrouss, A.M.; Ikki, S.S. Overview of precoding techniques for massive MIMO. *IEEE Access* **2021**, *9*, 60764–60801. [[CrossRef](#)]
9. Zhang, J.; Björnson, E.; Matthaiou, M.; Ng, D.W.K.; Yang, H.; Love, D.J. Prospective multiple antenna technologies for beyond 5G. *IEEE J. Sel. Areas Commun.* **2020**, *38*, 1637–1660. [[CrossRef](#)]
10. Ngo, H.Q.; Ashikhmin, A.; Yang, H.; Larsson, E.G.; Marzetta, T.L. Cell-free massive MIMO versus small cells. *IEEE Trans. Wirel. Commun.* **2017**, *16*, 1834–1850. [[CrossRef](#)]
11. Mai, T.C.; Ngo, H.Q.; Duong, T.Q. Downlink spectral efficiency of cell-free massive MIMO systems with multi-antenna users. *IEEE Trans. Commun.* **2020**, *68*, 4803–4815. [[CrossRef](#)]
12. Galougah, S.S.; Masoumi, H.; Emadi, M.J. User management in cell-free massive MIMO systems with limited fronthaul capacity. In Proceedings of the 2021 29th Iranian Conference on Electrical Engineering (ICEE), Tehran, Iran, 18–20 May 2021; IEEE: Piscataway, NJ, USA, 2021; pp. 853–858.
13. Shakya, I.L.; Ali, F.H. Joint access point selection and interference cancellation for cell-free massive MIMO. *IEEE Commun. Lett.* **2020**, *25*, 1313–1317. [[CrossRef](#)]
14. Wang, J.; Wang, B.; Fang, J.; Li, H. Millimeter wave cell-free massive MIMO systems: Joint beamforming and AP-user association. *IEEE Wirel. Commun. Lett.* **2021**, *11*, 298–302. [[CrossRef](#)]
15. Wu, Q.; Zhang, R. Towards smart and reconfigurable environment: Intelligent reflecting surface aided wireless network. *IEEE Commun. Mag.* **2019**, *58*, 106–112. [[CrossRef](#)]

16. Zeng, S.; Zhang, H.; Di, B.; Han, Z.; Song, L. Reconfigurable intelligent surface (RIS) assisted wireless coverage extension: RIS orientation and location optimization. *IEEE Commun. Lett.* **2020**, *25*, 269–273. [[CrossRef](#)]
17. Zhang, Y.; Di, B.; Zhang, H.; Lin, J.; Xu, C.; Zhang, D.; Li, Y.; Song, L. Beyond cell-free MIMO: Energy efficient reconfigurable intelligent surface aided cell-free MIMO communications. *IEEE Trans. Cogn. Commun. Netw.* **2021**, *7*, 412–426. [[CrossRef](#)]
18. Alonzo, M.; Buzzi, S.; Zappone, A.; D’Elia, C. Energy-efficient power control in cell-free and user-centric massive MIMO at millimeter wave. *IEEE Trans. Green Commun. Netw.* **2019**, *3*, 651–663. [[CrossRef](#)]
19. Lan, M.; Hei, Y.; Huo, M.; Li, H.; Li, W. A New Framework of RIS-Aided User-Centric Cell-Free Massive MIMO System for IoT Networks. *IEEE Internet Things J.* **2023**, *11*, 1110–1121. [[CrossRef](#)]
20. Sharma, V.; Allu, R.; Singh, S.K.; Singh, K.; Duong, T.Q.; Tsiftsis, T.A. Robust Transmission Design in Multi-Objective RIS-Aided SWIPT IoT Communications. *IEEE Internet Things J.* **2024**. [[CrossRef](#)]
21. Shen, C.; Chang, T.H.; Wang, K.Y.; Qiu, Z.; Chi, C.Y. Distributed robust multicell coordinated beamforming with imperfect CSI: An ADMM approach. *IEEE Trans. Signal Process.* **2012**, *60*, 2988–3003. [[CrossRef](#)]
22. Shen, K.; Yu, W. Fractional programming for communication systems—Part I: Power control and beamforming. *IEEE Trans. Signal Process.* **2018**, *66*, 2616–2630. [[CrossRef](#)]
23. Dinkelbach, W. On nonlinear fractional programming. *Manag. Sci.* **1967**, *13*, 492–498. [[CrossRef](#)]
24. Ben-Tal, A.; Nemirovski, A. *Lectures on Modern Convex Optimization: Analysis, Algorithms, and Engineering Applications*; SIAM: Philadelphia, PA, USA, 2001.
25. Chen, Q.; Yang, K.; Jiang, H.; Qiu, M. Joint beamforming coordination and user selection for CoMP-enabled NR-U networks. *IEEE Internet Things J.* **2021**, *9*, 14530–14541. [[CrossRef](#)]
26. Yang, Z.; Chen, M.; Saad, W.; Xu, W.; Shikh-Bahaei, M.; Poor, H.V.; Cui, S. Energy-efficient wireless communications with distributed reconfigurable intelligent surfaces. *IEEE Trans. Wirel. Commun.* **2021**, *21*, 665–679. [[CrossRef](#)]

**Disclaimer/Publisher’s Note:** The statements, opinions and data contained in all publications are solely those of the individual author(s) and contributor(s) and not of MDPI and/or the editor(s). MDPI and/or the editor(s) disclaim responsibility for any injury to people or property resulting from any ideas, methods, instructions or products referred to in the content.